



# EMODnet



European Marine  
Observation and  
Data Network

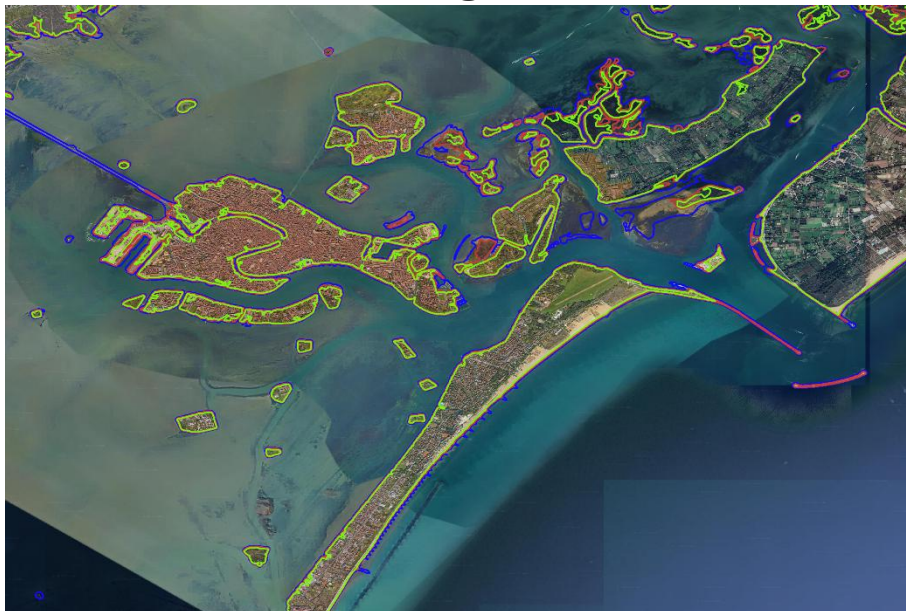
## EMODnet Thematic Lot n°1 – Bathymetry

EASME/EMFF/2019/1.3.1.9/Lot1/SI2.836043

Start date of the project: 20/12/2022 (24 months)

Centralisation Phase

### **D3.10 - Refined best estimate European digital coastlines for a range of vertical levels**



**January 2025**



## Disclaimer

The information and views set out in this report are those of the author(s) and do not necessarily reflect the official opinion of the CINEA or of the European Commission. Neither the CINEA, nor the European Commission, guarantee the accuracy of the data included in this study. Neither the CINEA, the European Commission nor any person acting on the CINEA's or on the European Commission's behalf may be held responsible for the use which may be made of the information.

## Document info

Title (and reference)	Refined best estimate European digital coastlines for a range of vertical levels
WP title (and reference number)	WP3
Task (and reference number)	D3.10 – Refined best estimate European digital coastlines for a range of vertical levels
Authors	Martin Verlaan, Rodrigo Socorro
Dissemination level	Public
Submission date	01/02/2025
Deliverable due date	31/10/2024
Version	4.0

# Table of Contents

<b>Summary</b> .....	<b>1</b>
<b>Disclaimer</b> .....	<b>2</b>
<b>1 Introduction</b> .....	<b>3</b>
<b>2 Methods</b> .....	<b>4</b>
2.1 Surface water detection from multispectral images .....	4
2.2 Method for the coastline estimation from optical satellite images.....	6
2.3 Linking water occurrence to tidal level.....	8
2.4 Coastline detection at high latitudes .....	10
2.5 Coastline detection in the Caribbean .....	14
<b>3 Post-processing and generation of final products</b> .....	<b>16</b>
3.1 Export of WaterIndex grids per tile .....	17
3.2 Filtering steps .....	18
3.3 Computing coastlines .....	21
3.4 Dataset for Caribbean.....	22
<b>4 Coastline comparison</b> .....	<b>22</b>
4.1 European continent.....	22
4.2 High latitudes.....	24
4.3 Comparison Caribbean .....	26
<b>5 Conclusions and recommendations</b> .....	<b>27</b>
<b>6 References</b> .....	<b>29</b>
<b>7 Annex – digital satellite derived coastlines and intertidal areas</b> .....	<b>30</b>

## Summary

EMODnet Bathymetry, started in 2009, aims to provide overview and access to available bathymetric datasets and to a harmonised digital bathymetry (DTM) for Europe's sea basins.

In 2018, a new set of satellite derived coastlines was added to the products of EMODnet bathymetry. The coastlines are given for the three most commonly used levels, i.e. Lowest Astronomical Tide (LAT), Mean Sea Level (MSL) and Mean High Water (MHW). In addition, the inter-tidal area is derived as the area between the coastlines at MHW and LAT. This dataset has been updated and refined in 2020 and 2022. This report describes the latest updates for the 2024 release.

The satellite derived coastlines and inter-tidal areas have been added as an extra Bathymetry layer in the EMODnet Central Viewing Service service<sup>1</sup>, which allows users to view these and also to download as digital files in shape format<sup>2</sup>. The layers have also been included in the WMS – WFS service<sup>3</sup>.

The main changes for this release are related to a redesign of part of the processing chain. Previously, the postprocessing and quality checks were performed using the coastline features. Over time it became clear that many tasks are slow and/or difficult for this type of data. Therefore, the postprocessing now works on the gridded data (at about 10m resolution) and the conversion to polygons is performed as the last step. This allows for much better postprocessing. However, since this is a big change to the processing software, not everything is optimal yet. The main remaining issues are that some lakes and canals are still seen as sea, Svalbard is still missing since this cannot be based on optical imagery alone. Deltares will work on further improvements for the next release (ie 2026).

---

<sup>1</sup> <https://emodnet.ec.europa.eu/geoviewer/>

<sup>2</sup> [https://downloads.emodnet-bathymetry.eu/v12/EMODnet Bathymetry 2024 coastlines.zip](https://downloads.emodnet-bathymetry.eu/v12/EMODnet_Bathymetry_2024_coastlines.zip)

<sup>3</sup> <https://emodnet.ec.europa.eu/geonetwork/srv/eng/catalog.search#/metadata/be8828f0-9390-4e5d-8f30-6831463d4d4b>

## Disclaimer

The EMODnet satellite derived coastline is a high-resolution geography data set (polyline) that must be considered as an estimate of the location of the coastline generated from a methodology involving optical satellite data and tidal modelling. Although the generation of the product has been done with the utmost care, both elements of the methodology might locally generate imprecise results leading to an inaccurate positioning of the resulting coastline.

In consequences as user of this product, you agree that:

- EMODnet Bathymetry does not provide warranties of any kind express or implied, about the completeness, accuracy, reliability, suitability or availability with respect to the information, products, services, or related graphics for any purpose. Any reliance you place on such information is therefore strictly at your own risk.
- In no event will EMODnet Bathymetry be liable for any loss or damage of any sorts arising from the use of this data and derivatives.
- The provided coastlines datasets do not serve as replacement of official coastlines as produced by the responsible national authorities. They should not be used where official coastlines are required.

## 1 Introduction

A coastline is a delineation materialised by a curve that separates the land from the sea. Since, the sea-level changes over time through tides and the weather, the instantaneous coastline also changes continuously. For many applications it is more practical to use the coastline at high-water, since this quantity is more stable and it reflects roughly what many people intuitively would consider the coastline. There are many different definitions of high-water but it is common practice to use Mean High Water for this purpose. On the other hand, for territorial claims, it is more common to base these on low water. For this purpose, it is common to use Lowest Astronomical Tides (LAT) (United Nations Convention on the Law of the Sea, 1994). To stay close to common practice, this report and the derived products will adhere to these conventions. This will also facilitate the comparison to other datasets. It should be noted that the term 'coastlines' is often used in a specific context where there are legal implications, in this context one implicitly refers to the official datasets as produced by the authorities. The datasets described here should not be used for this purpose. On the other hand, the satellite derived coastline described in this report uses a single methodology everywhere, ensuring a uniform generation of this product across Europe and thus can be used to compare with other coastline data. In addition, it can be useful where no other high-resolution coastline is available. Moreover, this methodology benefits from the fact that satellites revisit the same area frequently (e.g. sentinel 2 has a revisit frequency of around 2 days on average) allowing for frequent updates (in case of coastal erosion or anthropic effects) and for detection of tidal influences.



Figure 1 Example of coastlines at low-water, mean sea-level and high-water near IJmuiden in the Netherlands

This document describes the work related to satellite derived coastline that has been carried out within the EMODnet-Bathymetry projects. The first part of the document describes the

methodology for coastline retrieval. The following section presents the tidal correction methodology. Finally, the results and the conclusions are presented.

## 2 Methods

The identification of a “coastline” involves two general stages: the first requires the selection and definition of a coastline indicator feature, and the second is the detection of the chosen coastline feature within the available data source. To date, there are different techniques and algorithms for coastline detection. Recent photogrammetry, topographic data collection, and digital image-processing techniques now make it possible for the coastal investigator to use objective coastline detection methods. Some of the methods to be explored further are presented below.

### 2.1 Surface water detection from multispectral images

Existing methods for surface water detection from multispectral satellite data use the fact that water significantly absorbs most radiation at near-infrared wavelengths and beyond. This fact makes it easy to detect clear water employing spectral indices, such as the Normalized Difference Water Index (NDWI), McFeeters (1996).

$$NDWI = \frac{\rho_{green} - \rho_{nir}}{\rho_{green} + \rho_{nir}}$$

where  $\rho_{green}$  and  $\rho_{nir}$  correspond to the spectral reflectance of green and near-infrared bands. By design, the index values (similar to normalized difference vegetation index (Rouse Jr et al. (1974))) vary between -1 and 1, with water appearing mostly when the index value is greater than zero.



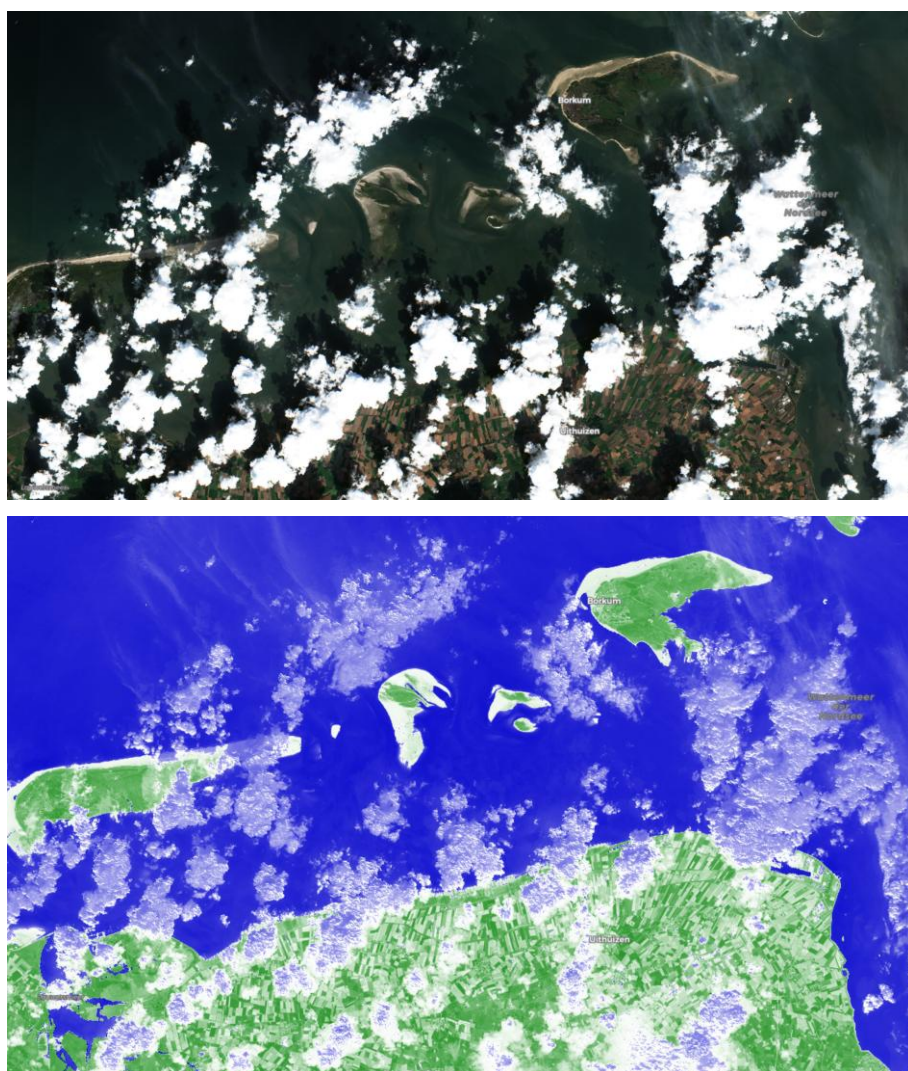


**Figure 2** Level 2 True color and NDWI images from Sentinel 2 on August 18th 2020 for Wadden Islands around Borkum in Germany

NDWI has been used to distinguish between land and water (Bayram et al, 2008; Kuleli et al, 2011; Almonacid-Caballer et al, 2016) and, hence, detect the coastline from satellite images. This technique was used for example in Donchyts et al. (2016) to study changes in land cover worldwide. The availability of Landsat satellite imagery allows us to study these coastlines from 1984 until now with a pixel resolution 15 to 30m. The recent Sentinel-2 satellite mission (ESA, 2016) even go up to a pixel resolution of 10m. Based on these images historic trends in coastal erosion can be detected. Several publication report on changes to coastlines, eg Luijendijk et al 2018. Similar analyses can be made to derive other coastal parameters such as vegetation (FAST, 2017), sand and human infrastructure.

Here, the NDWI algorithm is used to derive coastlines for the European waters and the Caribbean, this in combination with a tidal model allows, to retrieved coastlines at different vertical datum (e.g. MSL, MHW, LAT).



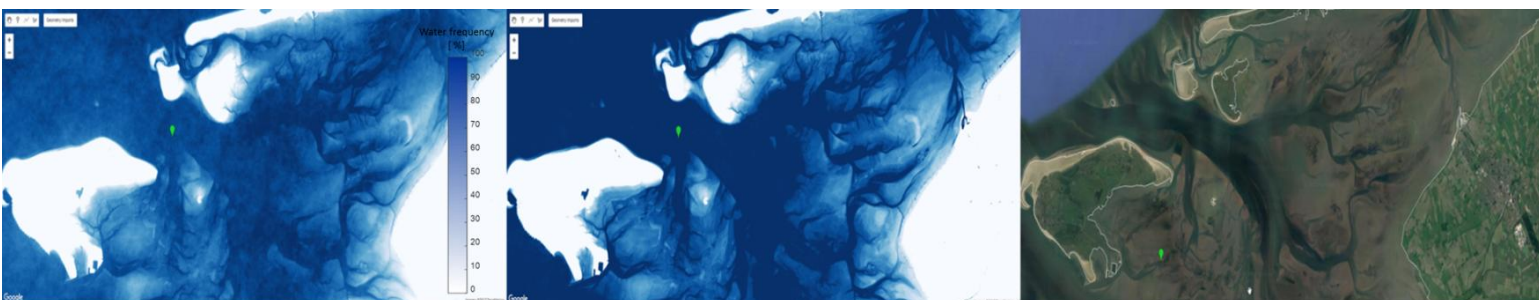


Figure 3 Water occurrence estimated from Landsat 8 and Sentinel-2 images around Wadden Island Borkum (Germany), the first image shows the water occurrence computed as a simple mean NDWI value from all images, the second image shows water occurrence estimate using statistical cloud removal method, and the third image the MHW coastline retrieved from water occurrence.

## 2.2 Method for the coastline estimation from optical satellite images

While a single satellite image can be used to detect coastline geometry, a much more robust approach is to combine many satellite images. This allows capturing not only coastline geometry, but also variations in the coastline geometry due to tidal water level changes. Several methods have been proposed to capture this variation in order to derive inter-tidal bathymetry (Sagar, 2017).

Processing of satellite images at large spatial and temporal scales is a computationally task, due to large volumes of satellite data to be processed, but also, due to variety in the satellite data radiometric properties and formats. In this project, the Google Earth Engine platform (Gorelick, 2018) has been used to overcome some of these challenges. The platform allows parallel processing of huge volumes of satellite data in reasonable time and harmonizes satellite data acquired by different satellite missions performed by NASA and ESA. In this project, a mixture of top-of-atmosphere reflectance satellite images from NASA/USGS Landsat 8 and ESA Sentinel-2 satellite missions, acquired during 2013-2020, has been used.

Automated detection of surface water from multispectral satellite images using passive sensor has received significant attention in recent years, Donchyts, 2016 (a), (b)., Pekel, 2016. A number of algorithms were developed to make surface water detection fully automatic. The main sources of noise for optical images are:

- Clouds and cloud shadows
- Shadows due to topographic effects
- Atmospheric effects (scattering, aerosols)
- Urban areas (complex spectral signal resulting in false-positive surface water)
- Snow and ice
- Systematic errors (georeferencing and georectification, sensor hardware or software errors, limited radiometric resolution)
- Variable thresholds for land/water discrimination when using classical NDWI spectral index
- Coastline with a very dynamic morphological changes
- Coastline with volcanic sand and rocks

To address most of these challenges, we have used statistical methods to process and combine many satellite images. In particular, instead of detecting surface water from satellite images using fixed NDWI threshold, the images were processed to represent a probability of land/water

boundary, a values close to 1 indicates that a particular pixel is always “wet”, therefore almost sure that location is water. The algorithm shown in Chapter 2 was used to process most images from Landsat 8 and Sentinel-2 missions covering EMODnet project area.

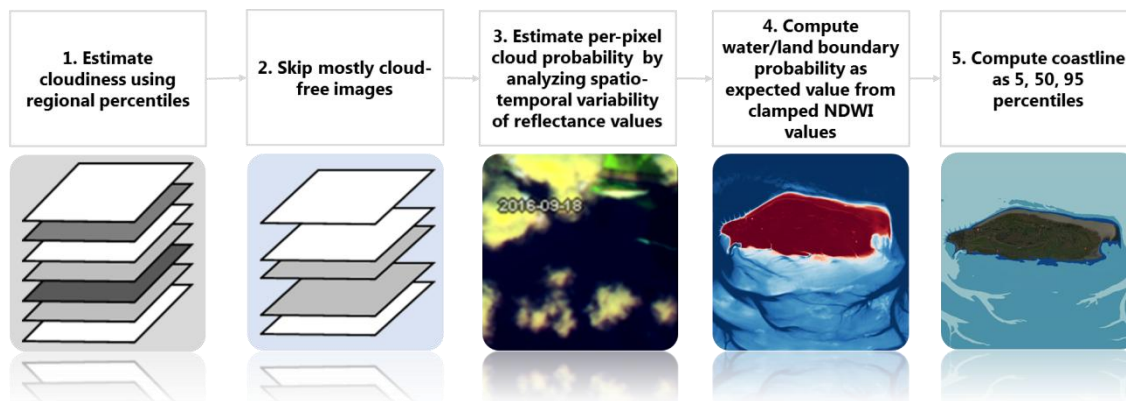


Figure 4 Processing pipeline for coastline detection from optical satellite images, capturing intertidal water level changes

Instead of performing a direct cloud masking for every image, the algorithm first “learns” the overall distribution of reflectance values within observed over every pixel as the first step. Then, a cloudiness metric is introduced for every image covering the area where potential coastline boundary is expected to be located. This metric is then used to filter-out images mostly covered by clouds. Then, a more robust per-pixel cloudiness probability is computed by comparing its values with the spatio-temporal distribution with a small neighbourhood around every pixel. The resulting cloudiness probability is used to estimate the final water occurrence, computed as the weighted average, using cloudiness as weights. The final water occurrence is used to estimate the coastline geometries.

After assigning cloudiness metric for every image (patch/tile), the algorithm uses mean cloud frequency estimated by Wilson, 2016 to determine the number of images to skip, significantly reducing noise in the resulting time series. For northern regions (The Netherlands, UK, Germany, Sweden, Finland), the mean cloud frequency is relatively high (~60-80%), resulting in only a fraction of satellite images can be used for processing. While this can be an issue for the analysis covering short periods, it was possible to overcome this using all of the available images acquired during 2013-2020.

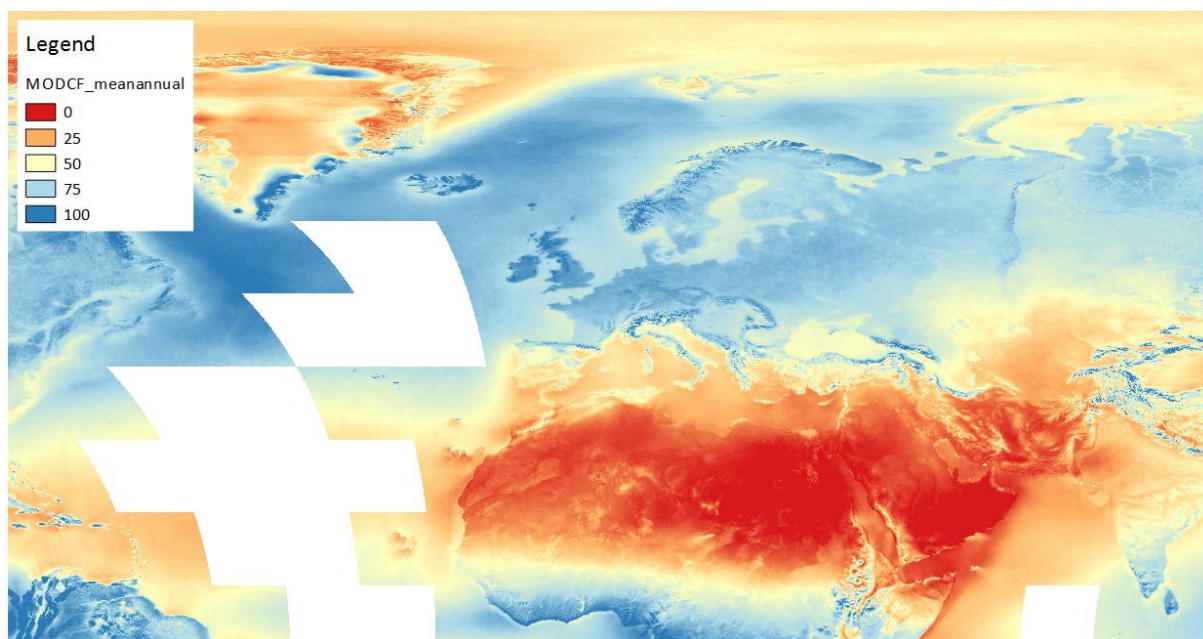


Figure 5 Cloud frequency (0-100) used during step 2 of the algorithm

Figure 6 shows an example of the final water occurrence estimated using the method outlined above. This spatial resolution of this water occurrence varies between 10m and 30m, depending on the number of Sentinel-2 and Landsat 8 images available for a given area and cloud conditions.

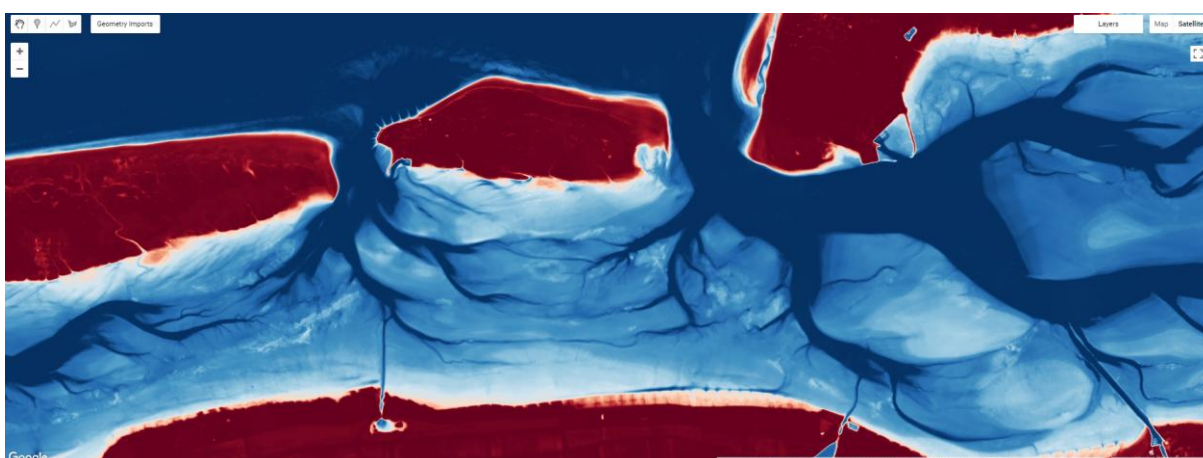


Figure 6 Water occurrence computed as expected value from all NDWI values, using per-pixel cloudiness values as weights (dark blue = permanent water, red = land).

### 2.3 Linking water occurrence to tidal level

In the introduction the coastline was defined as the physical interface between land and water, but this is also the most dynamic part of the coastal zone. Although much of the published literature have studied the problem of coastline position from multispectral images, only a few papers have addressed the problem of mapping the tide coordinated coastline.

Because of the dynamic nature of the ocean waters and of the near coastal lands the definition of an instantaneous coastline is introduced to point out that line position is relative to a given instant of time (Li et al., 2002). Thus, the coastline needs to be defined in a stable vertical datum in order to be used as a reference coastline. If this vertical datum is defined as the linear intersection

between the coastal surface and a desired water tidal level, the coastline is called tide-coordinated coastline (Li et al., 2002).

The tidal amplitudes are often amplified near the coast, while at the same time the spatial variability increases because the tidal wave propagation slows down in shallow waters. Tides are small in some regions but can also reach extremes of 13 meters in the Bristol Channel or 12.3 meters in Bay of the Mont Saint Michel, for example. Traditionally, corrections for local sea level have been computed from local tide gauges or tidal forecasts. On a global scale the number of permanent tide gauges is not sufficient to interpolate to arbitrary locations. At the same time, satellite-based altimeter observations of sea level do not have a sufficient temporal and spatial resolution to be used directly for correction of dynamic variations of the sea-level

In this project, the correction for sea level variation is based on use of the Global Tide and Surge Model (GTSMv4.1), which provides instantaneous water level and tide levels with global coverage. To ensure sufficient resolution near the coast, an unstructured grid model is used (Wang et. al. 2022, Irazoqui et. al. 2018 and Kernkamp et. al. 2011).

As the accuracy of the coastline position extracted from satellite images depends on the range of tidal height at the satellite overpass time (Yu et al., 2011), it is important to link to the tidal height at the time of image acquisition. The availability of GTSM tidal information allows retrieving water level at any time and location and compute satellite derived coastline to a coordinated tide level. The availability of the conversion between these vertical reference frames makes it possible to connect data-sets using different vertical reference frames, and conversion to a reference frame of choice for the user. The schematization of the vertical datum referencing process is shown in figure 7.

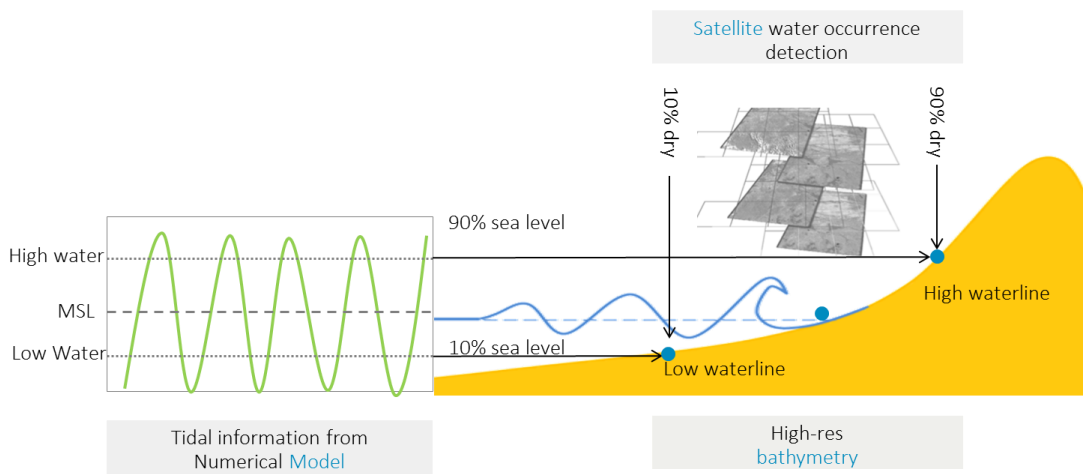


Figure 7 schematization of the vertical datum referencing of satellite derived coastline

Instead of linking to the water level for individual images the distribution of water occurrence and the distribution of the local water level were used to link both. Unfortunately, there was too much noise in the images near the extreme values of the water occurrence distribution, so the levels had to be limited to within the 5% to 95% range. The value of LAT is almost everywhere at a level of more than 95% water occurrence. In the end, it was decided to link LAT to 95%, MSL to 50% and MHW to 95% for the first version of this satellite derived coastline, to describe the maximum tidal range attainable at this time. Future work will aim at more accurate representation of MHW and more extreme levels. The water occurrence grids were contoured on a tile-by-tile basis.



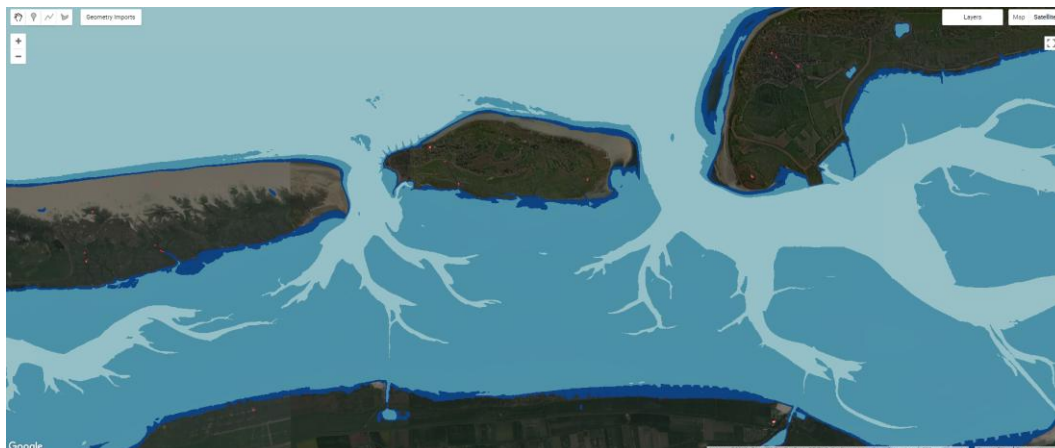


Figure 8 Coastline polygons for MHW, MSL, LAT estimated as 5%, 50%, and 95% percentiles of water occurrence images.

## 2.4 Coastline detection at high latitudes

Deriving coastline for Northern regions such as Greenland and Svalbard can be very challenging due to high cloud cover and the fact that land and water are frequently covered by snow and ice. Furthermore, deriving water/land boundary from optical images in these areas can result in false-positive water detection due to low sun elevation.

However, in recent years there was very little snow and ice end of summer, which makes detection of the coastline easier. In addition, Sentinel 1 radar images have been used to reduce the false positives.



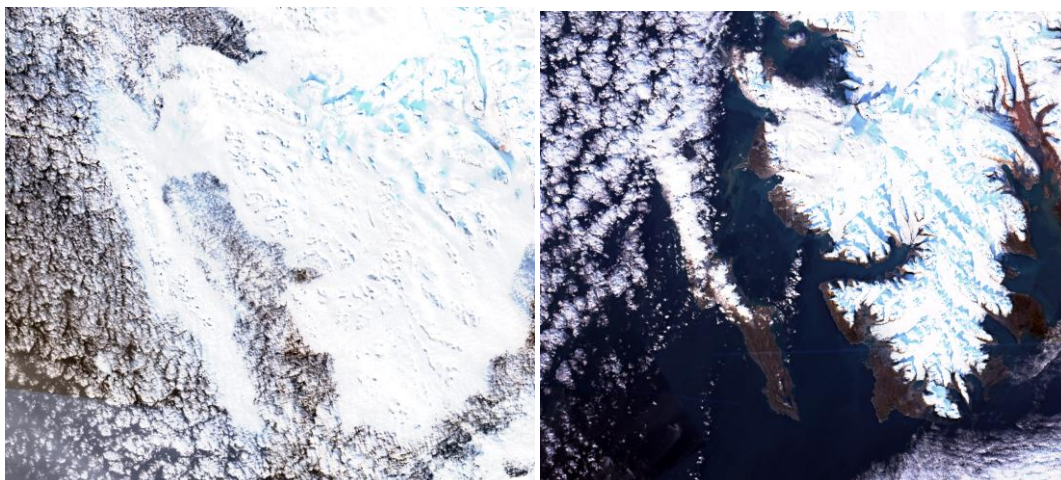


Figure 9 Sentinel 2 optical images of Western Svalbard on March 21 September 25, 2020.

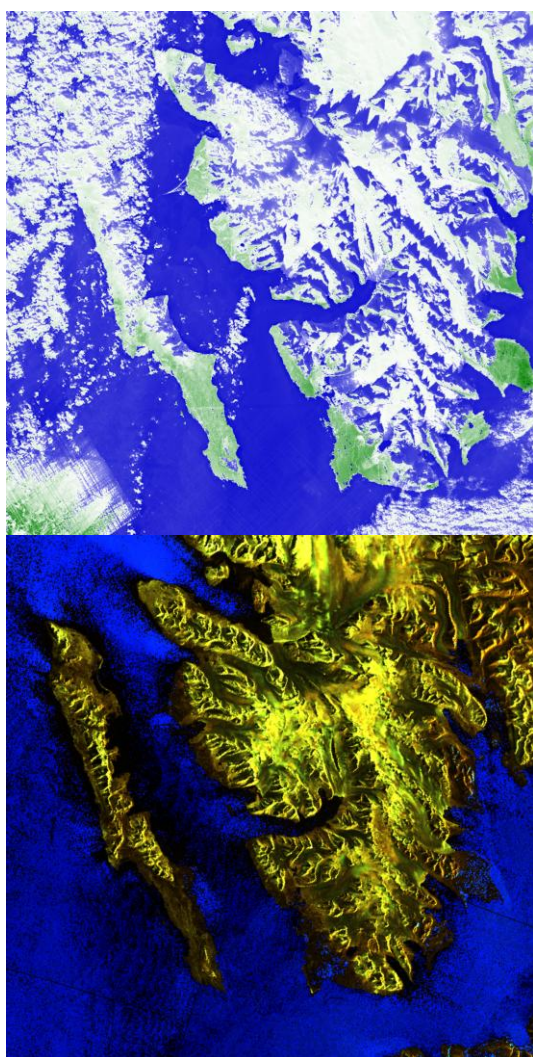


Figure 10 NDWI for Sentinel 2 on September 25 and Sentinel 1 SAR image on September 26, 2020

To overcome these challenges, it was decided to combine optical (Landsat 8) and SAR (Sentinel-1) images acquired only during summer months (June to September). All images acquired during these months are used in processing to generate input features for supervised machine learning algorithm Random Forest (Breiman 2001). The overall algorithm can be outlined in the following steps:

1. For every processing tile, generate input features by combining 100-1000 summer images of Sentinel-1 (HH, HV polarization), use 35% percentile, neighbourhood mean, std as input features
2. For every processing tile, generate input features by combining 100-1000 least-cloudy Landsat 8 images, use 10% percentile, std as input features
3. Generate weak labels using stratified sampling and OpenStreetMap coastline as land use classes, use 1. and 2. as input features
4. Train the first Random Forest classifier with the output = PROBABILITY
5. Remove confusing input samples by analysing probability histogram
6. Train the second Random Forest classifier with the output = CLASS
7. Generate the final coastline

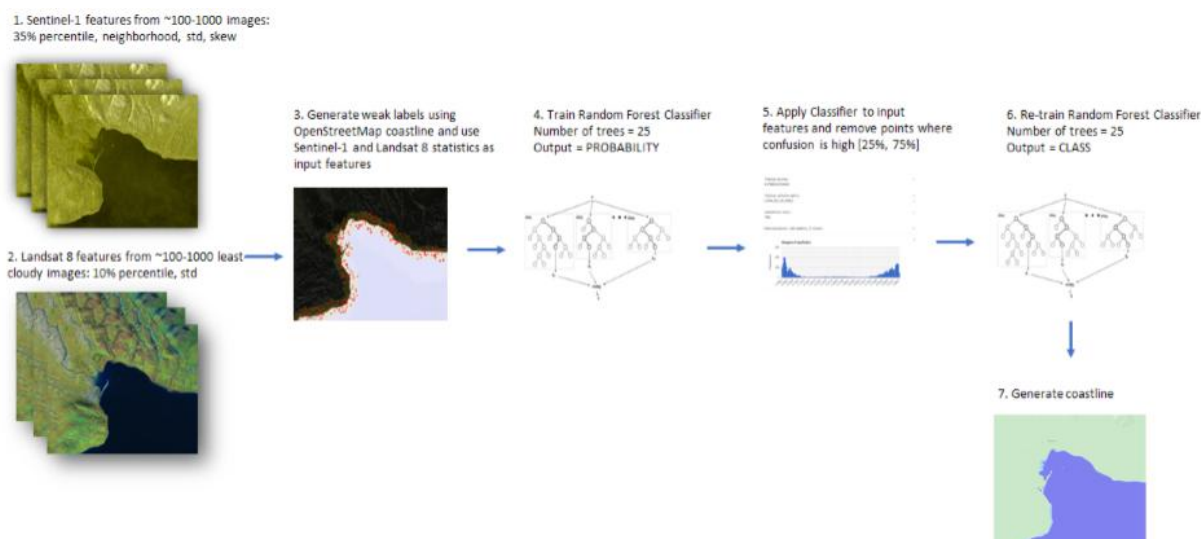


Figure 11 Workflow of the semi-supervised algorithm used to generate the coastline for Greenland, Jan Mayen and Svalbard from Sentinel-1 SAR and Landsat 8 optical data

The resulting coastline shows a very high performance, but still required manual checks to eliminate false land detecting in the areas where number of satellite images is low or where confusion is very high (e.g. water areas always covered by moving ice or very steep hilly areas).

Next the coastline was generated from the raster classification to vector format at 10m resolution. Several additional steps were applied to ensure quality of the results, such as:

- Overriding pixel classes as deep water (EMODnet < -50m), as shown in Figure 12
- Overriding pixel classes as land for high elevation pixels (ALOS DEM > 50m)
- Manual overriding of pixels to be water or land based on visual inspection
- Fallback to OpenStreetMap coastline for the most Northern regions, Figure 13

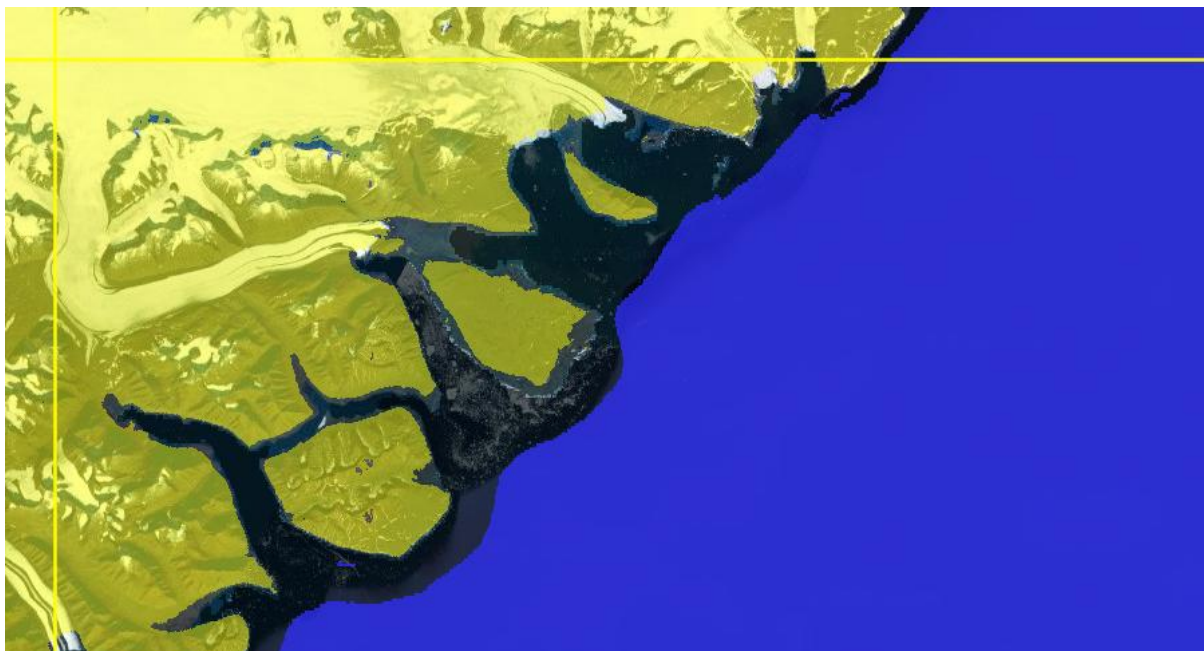


Figure 12 The classified coastline was combined with EMODnet to remove some of off-shore false-positives created by floating ice, all pixels where water depth is  $< -50\text{m}$  were classified as water. Correspondingly, all pixels where the ALOS DEM was higher than  $50\text{m}$  were classified as land.

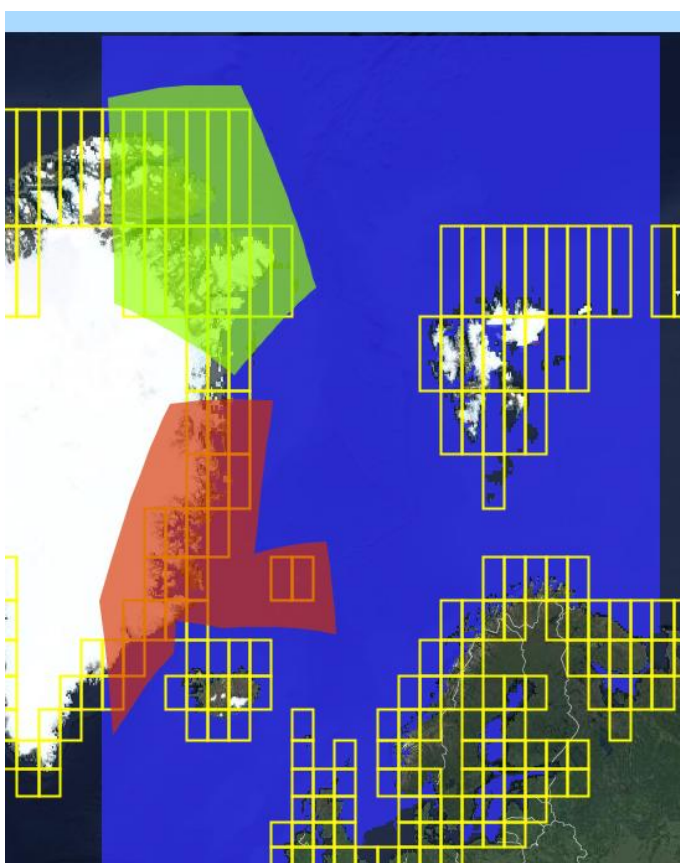


Figure 13 Greenland tiles where OpenStreetMap was used to extract coastline (green) and where Random Forest based algorithm was applied (red)

It's important to note that the Northern regions marked green in Figure 13 are much smaller than they seem, because the area is stretched by the Web Mercator projection used for visualization.



The fallback to the OpenStreetMap coastline was applied only to the tiles where ice was present on almost all optical or SAR images, like shown in Figure 14, where some of the areas are misclassified as land due to permanent ice present in all images. Further improvements may be possible in future versions of the classification scheme, but at the moment too many false islands are generated.

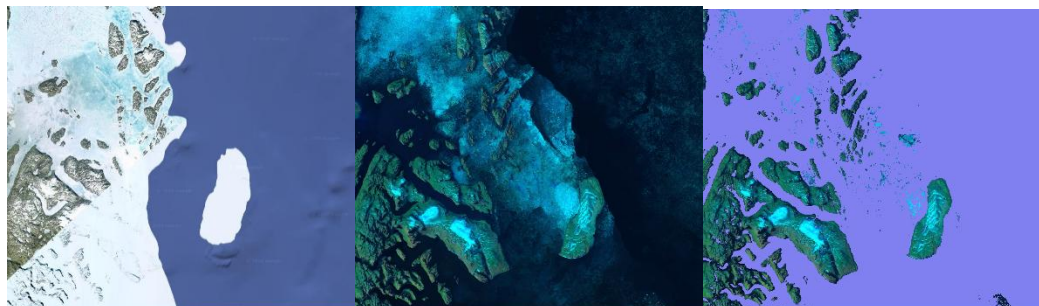


Figure 14 Comparison of Google base map (left), Landsat 8 5% TOA reflectance composite (middle), and reconstructed coastline (right). Some areas with almost always permanent ice present on the sea surface are still classified as land.

For the Arctic regions, separate low and high-water coastline were not derived, since limiting the images to summer only in combination with the poor lighting and high cloud cover leaves too few images for this type of analysis. Fortunately, much of the coastline in this region shows only a small inter-tidal zone. This implies that in the final coastlines the data for low-, mean- and high-tide will coincide.

The coastline at high latitudes has not been updated in the 2024 release. However, a copy has been included with the 2024 release.

## 2.5 Coastline detection in the Caribbean

In the 2022 release of the EMODnet satellite derived coastline, the Caribbean was included for the first time. In this release the coastlines were based on the same satellite imagery, but the post-processing has been changed, as described in section 3. In large parts of the Caribbean the water is clear and land-water detection works well. The processing uses the same methods as for European continental waters. However, in some parts in the southern Caribbean something like water vegetation or silt is mistaken for land sometimes. There are other exceptions, such as the salt works in Bonaire. These basins contain a thin layer of seawater that is evaporated to produce salt. The algorithm correctly classifies these pixels as water, but it's not part of the sea of course. However, due to the proximity of the sea the coastline estimates are affected here.

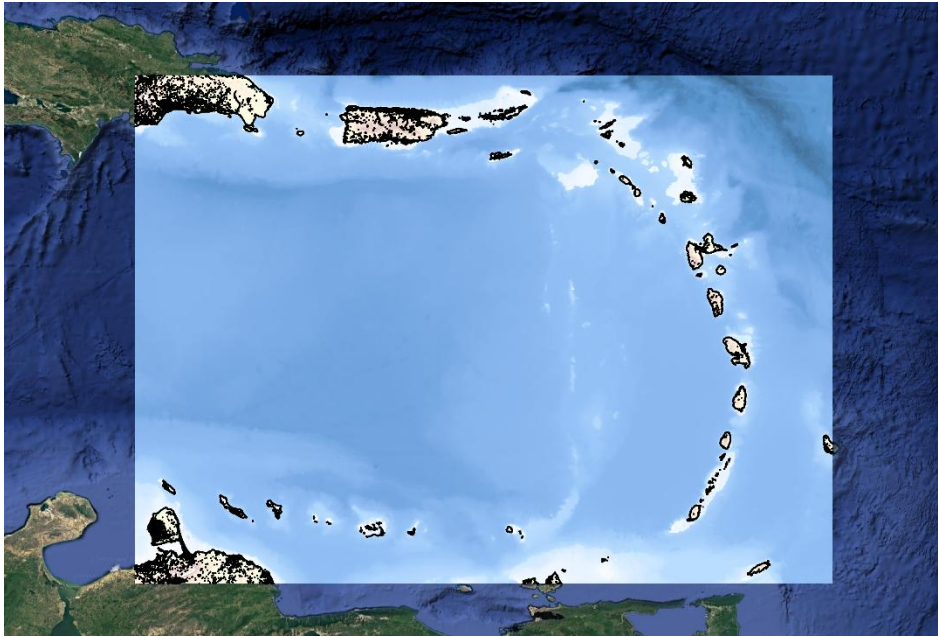


Figure 15 Overview of Caribbean area with coastlines in black.

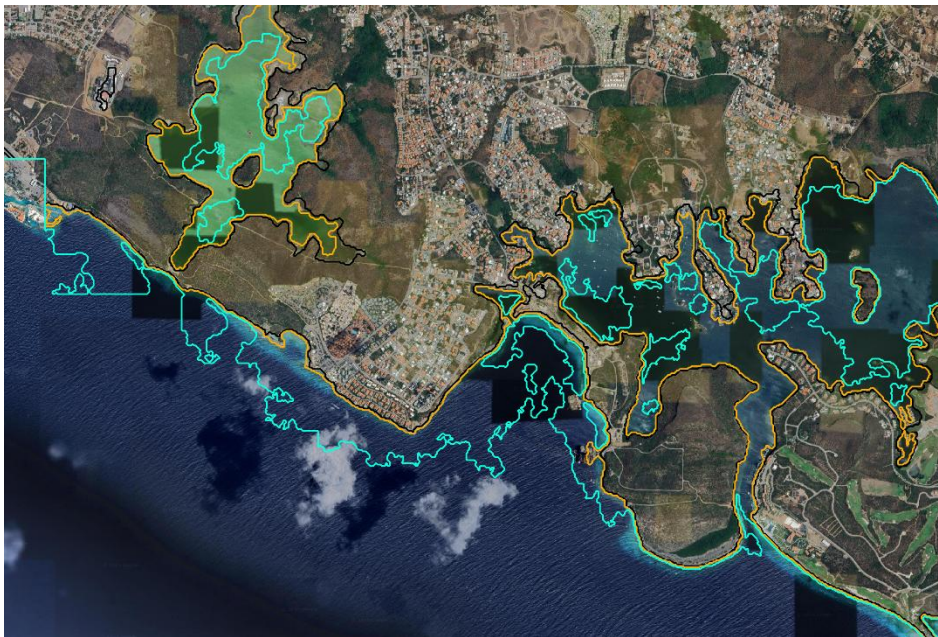


Figure 16 Example where the low-water coastline is not detected well (southern Curacao)





Figure 17 Salt works in Bonaire

### 3 Post-processing and generation of final products

After land-water detection and contouring, as described above, there are still several steps needed to produce a final set of products. These computations have been revised completely since the previous release. The largest difference is that previously the postprocessing started with polygons, but working with large polygons turned out to be difficult and slow. Therefore, the postprocessing now starts with an export of the WaterIndex (WI).

While post-processing gridded data is easier, a complete new set of routines were needed. Moreover, the grids involved are large, eg 868291 by 623389 for the European continent, so parallel processing and out of memory processing is needed.

The postprocessing steps can be divided into three groups: export of gridded WaterIndex, filtering of the data, and finally contouring of the data. The next few sections describe these steps in more detail.

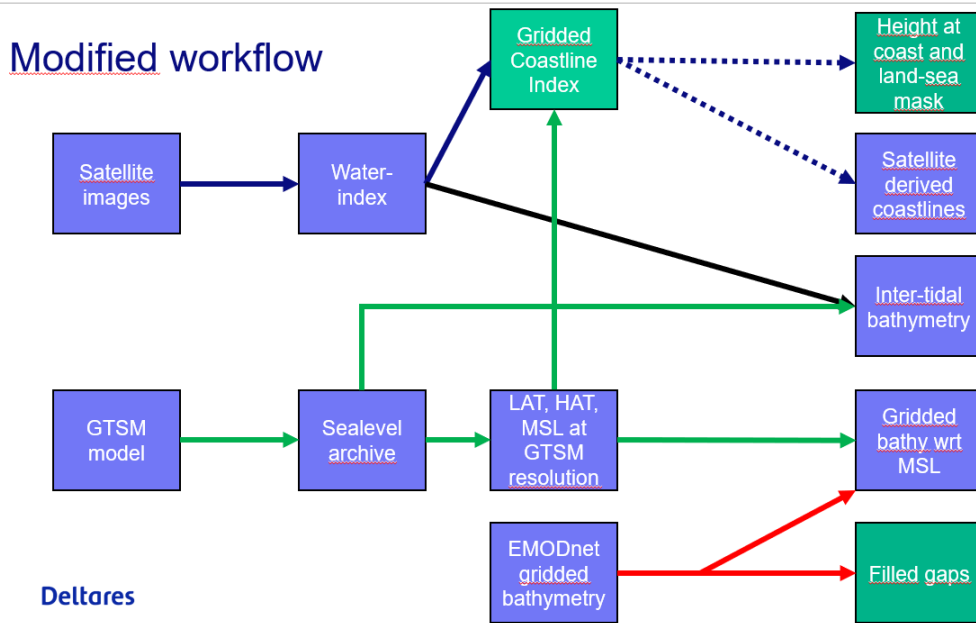


Figure 18 Modified workflow for Satellite Derived Coastlines

### 3.1 Export of WaterIndex grids per tile

After processing optical satellite data to the level of water-index that together cover the water as detected, the data were exported. Since the GEE computations were organized in small rectangular areas to facilitate parallel computation, this resulted in many files. The figure below gives an overview of the division into tiles. Each tile has an ID, i.e. the number also shown in the figure below. For efficiency, the tiles that consist entirely of land or entirely of water were excluded from the computations in GEE. For the coastline computations the water-index was converted to a class number, 0 for  $WI < 5\%$ , 1 for  $5\% < WI < 50\%$ , 2 for  $50\% < WI < 95\%$  and 3 for  $WI > 95\%$ . Figure 19 shows an example of this water-mask dataset. It is a gridded dataset with a resolution of about 10m.

The figures below show the exported tiles and an example of a gridded dataset for the WaterIndex. Even though many aspects of the coastline are correctly identified from the satellite imagery, there are also a large number of mistakes and missing points. The filtering steps aim to increase the accuracy of the data, by cross checking with other datasets.

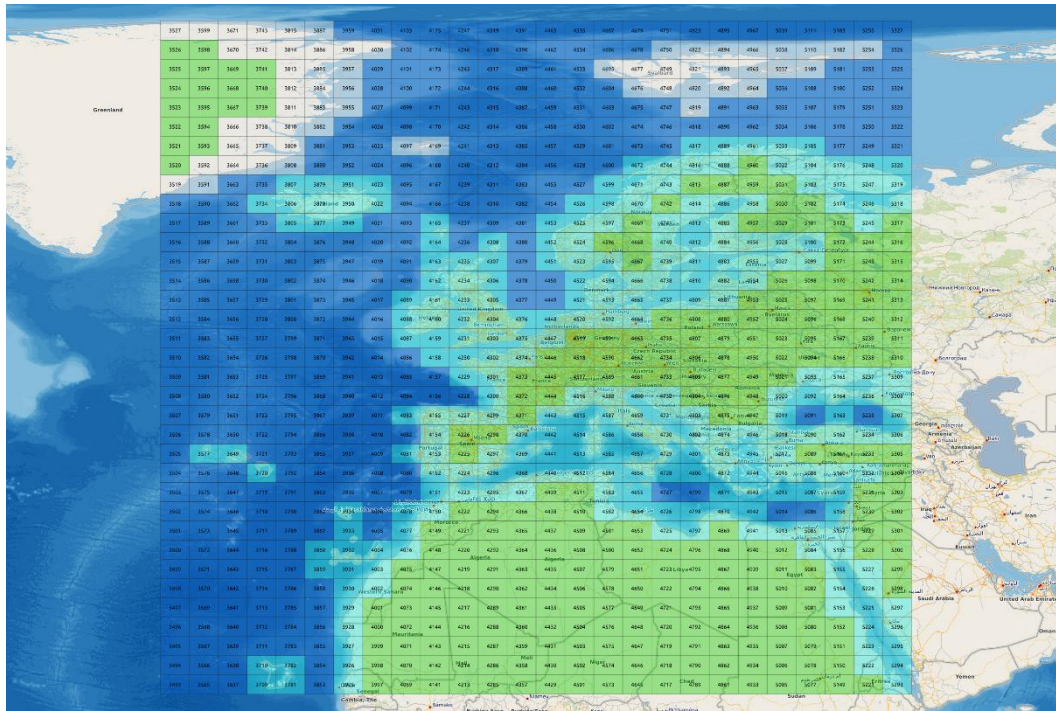


Figure 19 Tiles exported and their status: land only (green), water only (dark blue), part land/part water (light blue), combined optical-SAR detection (white)

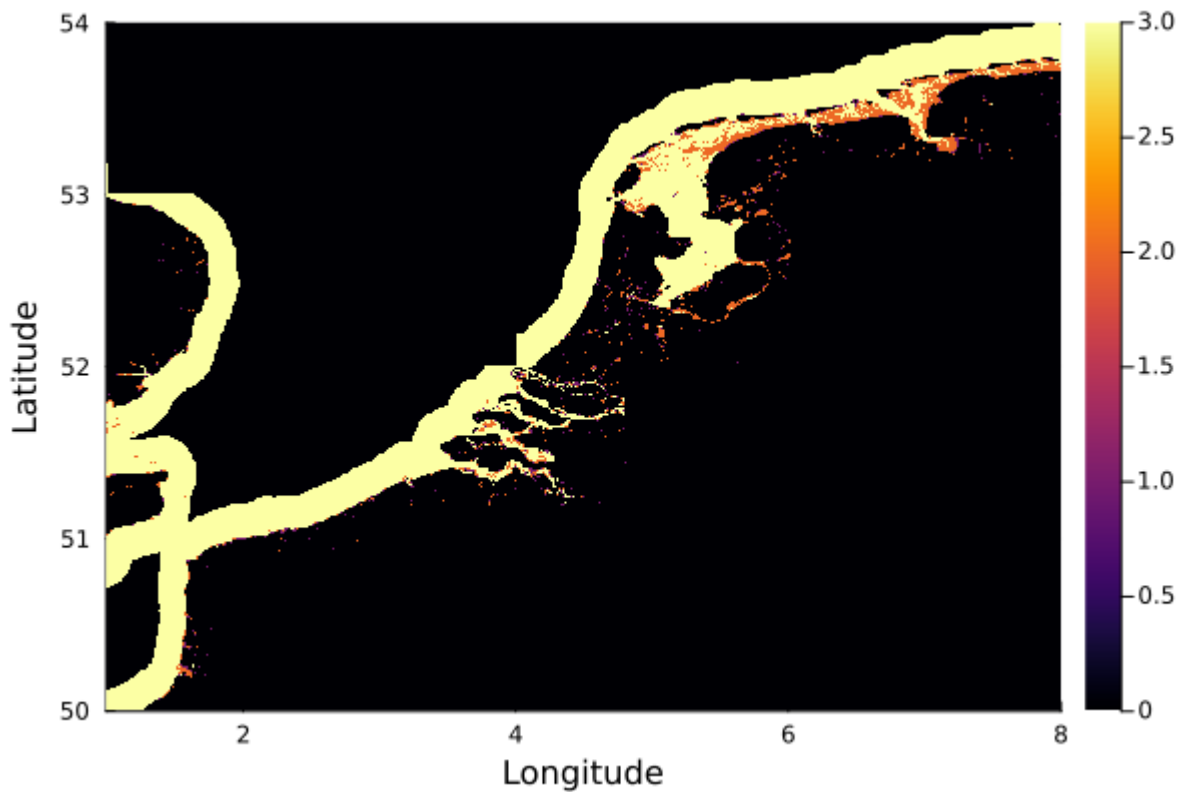


Figure 20 Example of raw water mask as exported from GEE

### 3.2 Filtering steps

The water detection algorithm does not distinguish between fresh and salt water, nor between coastal versus inland water, resulting in many lakes and other surface water to appear that are not considered to be part of the coastline. It may not be possible to create a clear separation in all

cases. The aim of the processing step described here is to eliminate smaller waters that are not connected to open sea. This eliminates many features. The filtering procedure and threshold have been designed to be conservative, i.e. not to delete waters that might be part of the coastline. This implies that the dataset will contain water-land boundaries that will not be considered to be part of the coastline.

The figure below shows part of the Netherlands before and after filtering of small disconnected waters. It can be seen that the North Sea Channel connecting the harbour of Amsterdam to the North Sea is connected to the North Sea in this data-set, but in reality there are sluices near the coast, that separate the water in this channel from the North Sea. Apparently, the sluice gates were not detected from the satellite images.

In the current release two filtering steps were applied to the WI data:

1. For water deeper than 20 meters in the EMODnet bathymetry the cells were set to water WM=3
2. A global land-sea-mask from NASA was used to create a distance to coast parameter. Cells with a positive distance larger than 30 cells were set to sea (WM=3) and cells with a negative distance smaller than -20 cells were set to land (WM=0). The original land-sea mask can be found at: <https://oceancolor.gsfc.nasa.gov/resources/docs/ancillary/>

The figures below illustrate these datasets and their influence on the resulting

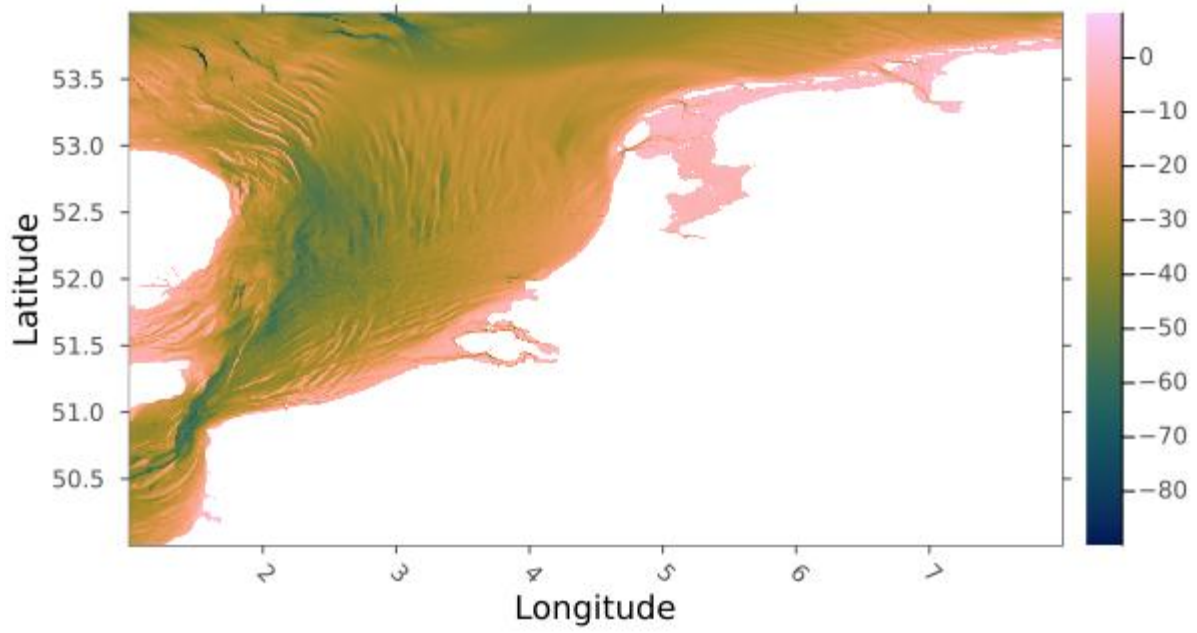


Figure 21 EMODnet gridded bathymetry

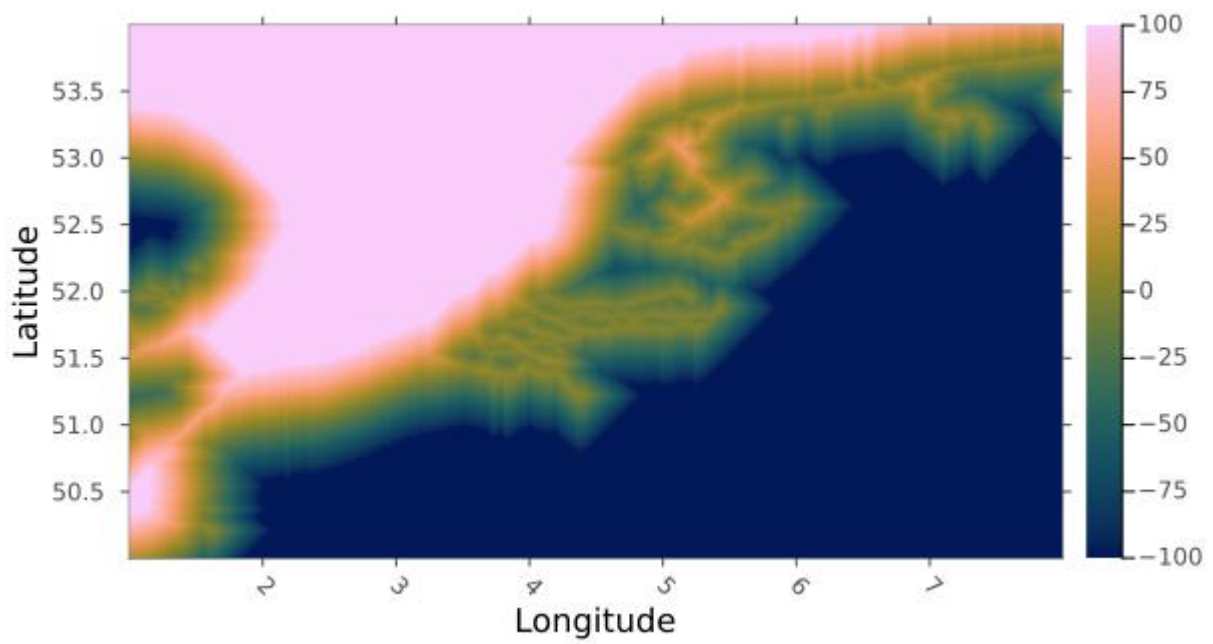


Figure 22 Distance to coast



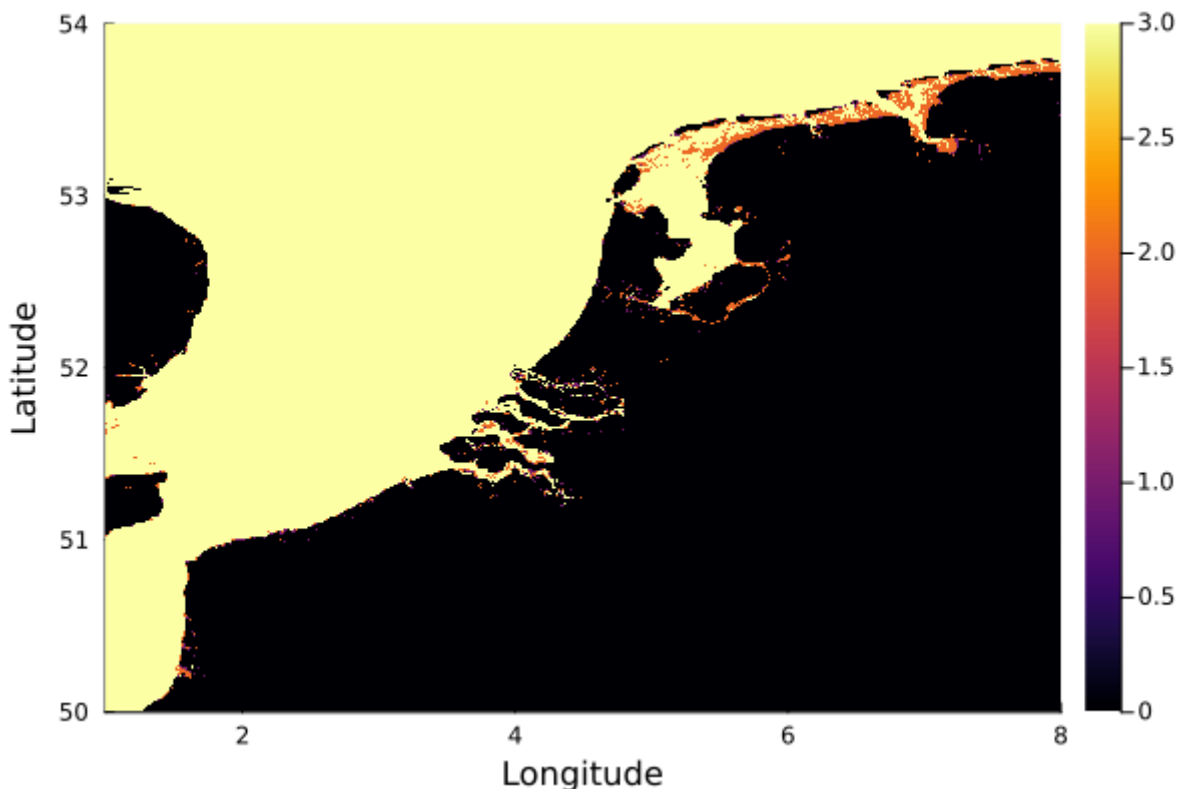


Figure 23 WaterMask, after application of the filters

### 3.3 Computing coastlines

Finally, the cleaned WaterMasks were converted to coastlines. This process is very similar to the computation of contour lines. The algorithm used is a bit different from the previous algorithm, which results in slightly different coastlines. In the previous algorithm all coastlines were either vertical or horizontal. In the new algorithm the coastline cuts through the middle between a selected point and a neighbouring point that is not selected. This results in 16 different topologies, where the coastlines can go in 8 different directions instead of 4 before.

Because the high-resolution, the amount of data to process was larger than fitted in memory. Therefore, the grid was processed in tiles. The process was optimized to exclude tiles that were all water or all land. Separate contouring was performed for Lowest Astronomical Tide (LAT), Mean SeaLevel (MSL), Mean High Water (MHW) and InterTidal Areas (ITA)

The figure below shows an example of the coastlines.



Figure 24 Plotted coastline as poly-line format for Heligoland (Final product delivered)

### 3.4 Dataset for Caribbean

The satellite derived coastlines for the Caribbean were collected into a separate dataset. The formats and processing were kept identical.

## 4 Coastline comparison

### 4.1 European continent

This section presents a visual comparison between the Satellite Derived Coastline (SDC), the coastline derived from Open Street Maps<sup>4</sup> (OSM) and the coastline provided by EMODnet project partners. The comparison has been performed with the 2022 release of the SDC, since the differences are expected to be small at these scales.

The OSM coastline has been derived from Open Street Map ways tagged with `natural=coastline`. This data contains all the detail available in OSM. For small scale maps (small zoom levels) it might be too detailed and therefore slow to use and not well readable. The OSM coastline projection is in WGS84 (EPSG:4326) or web Mercator (EPSG:3857). The coastlines can be obtained as lines and/or land polygons and/or water polygons.

Within the EMODnet-HRSM project, one task was to gather official coastlines for the European waters. Information about coastline has been gathered per country, the data comes in different

---

<sup>4</sup> Coastline in OSM is defined as the mean high water (spring) line between the sea and land (with the water on the right side of the way).  
[https://wiki.openstreetmap.org/wiki/Map\\_Features](https://wiki.openstreetmap.org/wiki/Map_Features)

coordinate system and at different spatial resolutions. This data set is also used for the visual comparison and we will refer to it as “Official Coastline”.

The visual examination after the retrieval process showed that the SDC coastline is generally in good visual agreement with OSM and the official coastline. The comparison suggests that the discrepancy between the SDC and the other data sets remains within the pixel size in sandy beaches. This comparison therefore bodes well for future attempts to detect coastline changes of larger magnitude than the pixel resolution (10 m).

There are areas where there is a bigger discrepancy between the SDC, OSM and the official coastline. For example, in areas under land reclamation or human intervention the coastline changes rapidly over time. Resolution and accuracy of OSM coastline is variable since it is the result of many contributions by many people and from many sources. In the other hand updates in the official coastline might not be as fast as the changes due to human interventions. To illustrate this example Figure 25 is presented. The figure shows Luka Ploce in Croatia, where SDC gives a more detailed contour of the Port in that area.

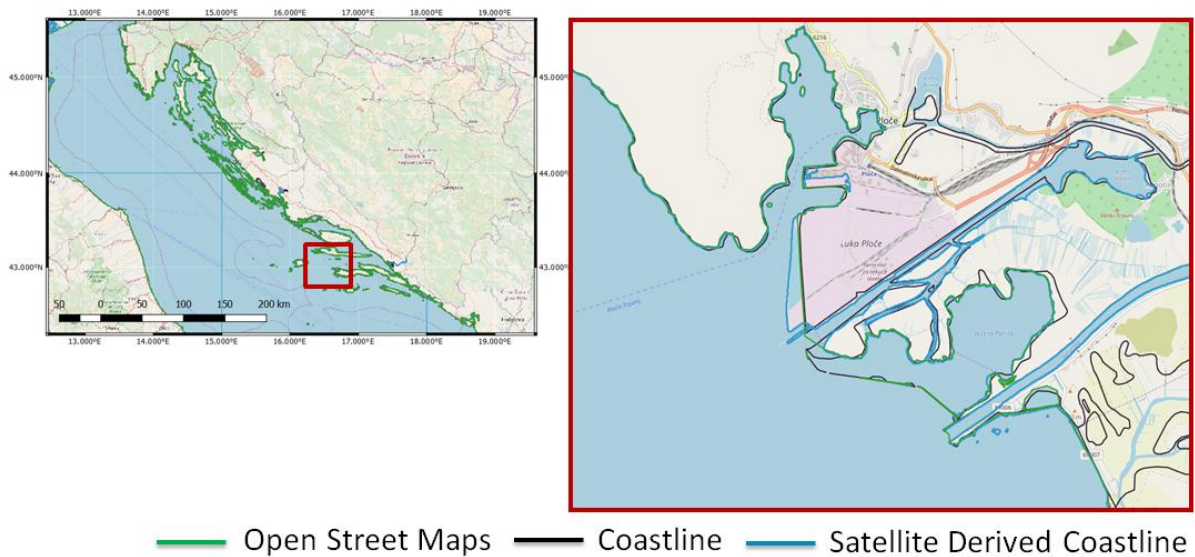


Figure 25 Croatia (Luka Ploce): comparison between SDC (high water), OSM and coastline from official sources

The fact that the biggest discrepancy while comparing the coastlines were consistently observed at intertidal areas, indicates that the current tide level, possible effects of storm surges and the beach slope, play an important role. Figure 26 presents the comparison between the different coastlines in an intertidal area. The chosen case is situated in the Netherlands. Terschelling is one of the islands situated in the Wadden Sea. This area is the largest unbroken system of intertidal sand and mud flats in the world. Morphodynamics is very active here, so the coastline changes rapidly. The beach is also very flat, so that small differences in approach lead to large spatial differences. The difference between the SDC, the OSM coastline and the official coastline can reach a difference up to 650 meters.



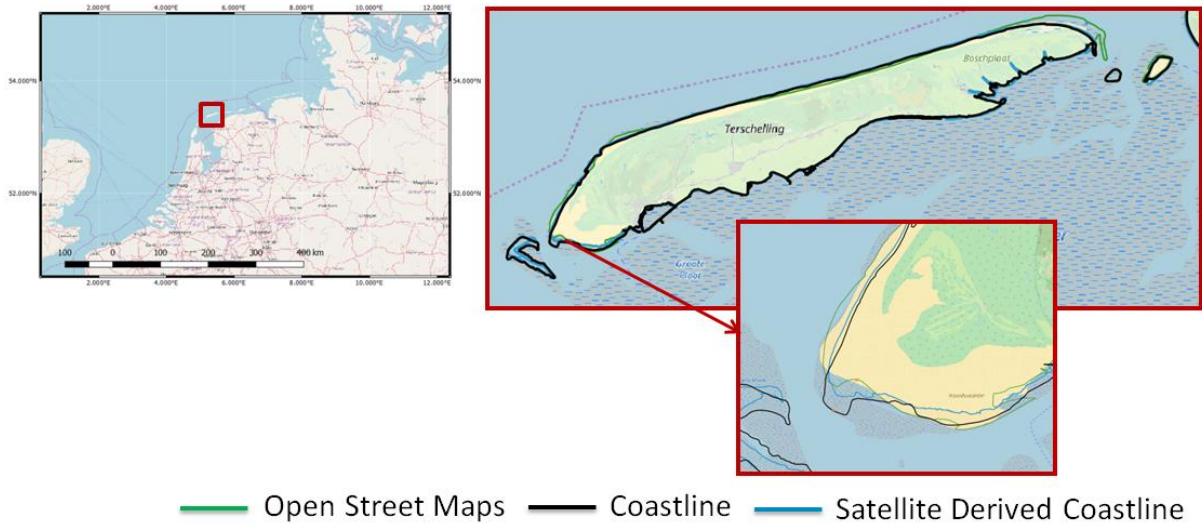


Figure 26 Netherlands (Terschelling): comparison between SDC (high water), OSM and coastline from official sources

Coastline has been defined as a line that forms the boundary between the land and the ocean. Nevertheless, in some regions that line cannot clearly be established. Precisely in those regions, the discrepancy between the SDC, the OSM coastline and the official coastline tends to increase. Figure 27 present a peculiar case in Portugal (Aveiro) where SDC provide more detailed information that OSM and the official coastline.

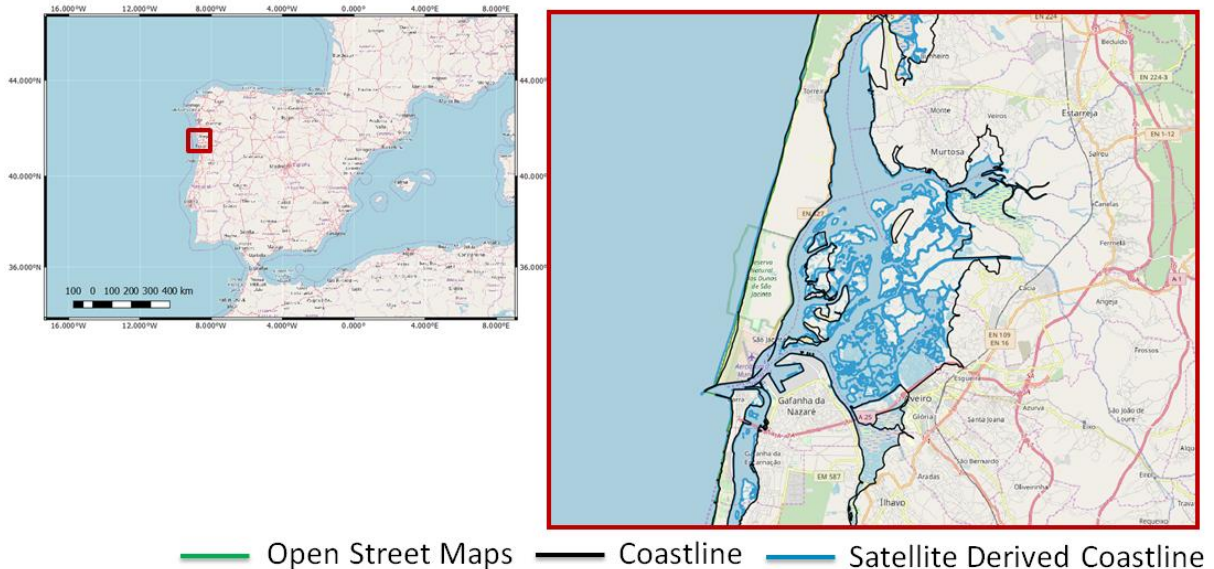


Figure 27 Portugal (Aveiro): comparison between SDC (high water), OSM and coastline from official sources

## 4.2 High latitudes

At high latitudes the performance of the new detection algorithm is generally good. Difficulties arise in some areas which combine frequent ice and high cloud cover rate. Note also that the edge of glaciers is dynamic and thus depends of the timing of the satellite images used. Meltwater from glaciers also introduces much sediment into the water, which makes detection harder.

The figures below compare the new method (green) against Open StreetMap (OSM red), with a Google satellite image as background.

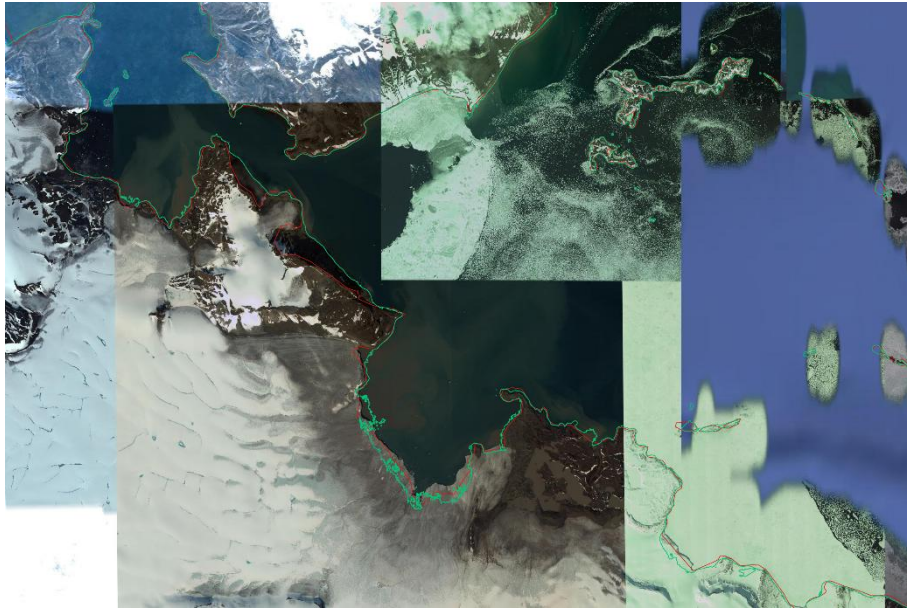


Figure 28 SDC (green) against OSM (red) for eastern Svalbard



Figure 29 SDC (green) against OSM (red) for eastern Greenland



### 4.3 Comparison Caribbean

Here the satellite derived coastlines for the Caribbean are briefly compared to the OSM coastline for some selected cases for illustration. Figure 30 Sample coastlines at Antigua (Open Streetmap in red) shows the estimated coastlines in comparison to OSM (red). In most parts the OSM coastline is a bit further inland. This could be close to a very visible high-water line that is only reached very infrequently.



Figure 30 Sample coastlines at Antigua (Open Streetmap in red)

Figure 31 Dominica with a cliff on northern side, below shows an example where a shadow from a cliff confused the land-water detection. OSM is also quite inaccurate here.



Figure 31 Dominica with a cliff on northern side

Figure 32 shows an example where a small mangrove was classified as and by the satellite derived coastline.

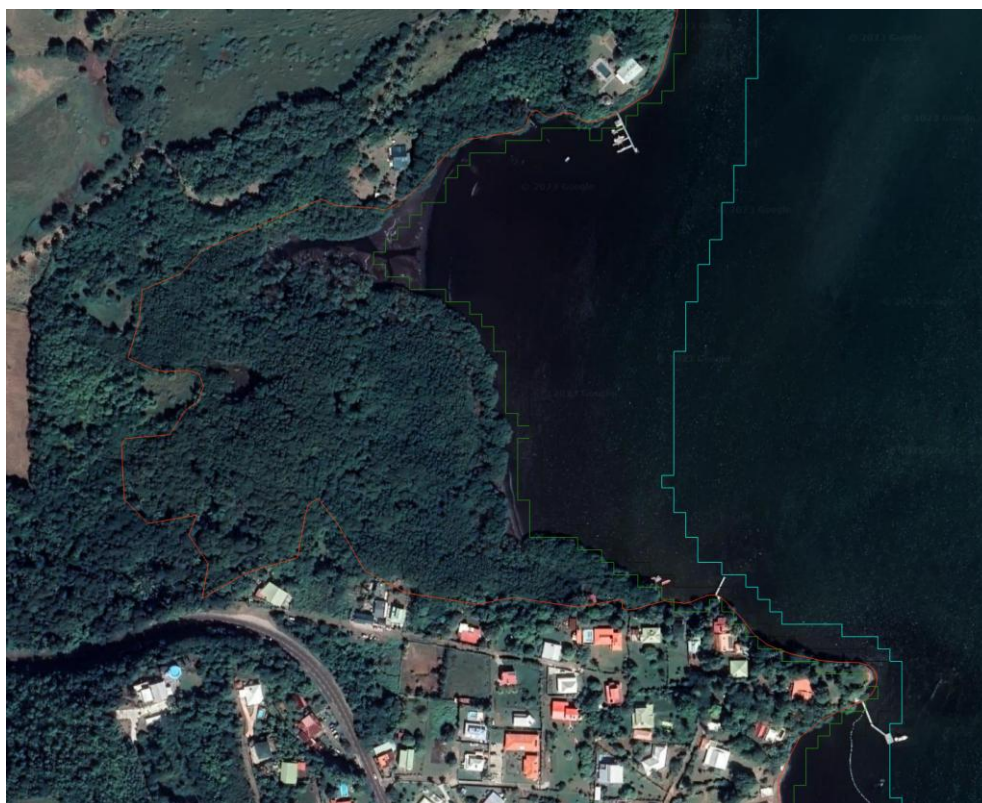


Figure 32 Example with mangrove

## 5 Conclusions and recommendations

In this report the methods are described which were used to derive a coastline from optical satellite imagery. In comparison to other sources, the coastline retrieved from satellite images shows good agreement in most areas. It is consistent with the Open Street Map (OSM) and the official coastlines, giving confidence that the interpretation of different positions of SDC shows a real representation of the coastline at different datum.

Although the quality is generally high, the following aspects could be improved:

- The current coastlines are given as poly-lines in the data files. Representation as polygons, i.e. contours around the sea, would allow for a larger range of applications, since the additional topology allows e.g. to determine if a point is in the sea, or overlaps and many other operations.
- The new post-processing was generally successful, but still shows numerous lakes when they're close to the coast. Further refinements of the filtering steps can potentially improve this. As this is the first release using the new post-processing, not all issues may be known and improvements are likely to be needed.
- An advantage of the new post-processing with gridded WaterMasks makes it easier compare to the land-sea mask of the gridded bathymetry and work towards improving the consistency.

Only part of the recommendations from the previous releases have been resolved. Some of the remaining issues are:

- At high latitudes, there are a few areas with too few useful images, resulting in some ice to be classified as small islands. Even with the current quality checks not all were removed. Improvement is desirable in future versions.
- So far it was not possible to detect the coastline at low water for Iceland and the Faroe Islands. Perhaps the very high cloud cover and poor lighting conditions are to blame. This needs further investigation.
- NDWI is not robust for very turbid water. In the future, the analysis might be extended to use MNDWI and maybe other indices to improve quality for these regions (in particular, UK) is needed.
- Shadows at steep coasts and spray in the surf zone is sometimes accidentally classified as land.
- A further exploration and improving of the algorithm in urban areas is needed. For example, construction activities during the period of the analysis may lead to misclassification of these areas as inter-tidal.
- The low-water coastline seems quite noisy in several locations. Perhaps the detection thresholds need to be adjusted here.
- The land-water detection algorithm is confused by several coastal features, such as cliffs, wave breaker zones and vegetation



## 6 References

1. Breiman, Leo. "Random forests." *Machine learning* 45.1 (2001): 5-32.
2. Convention on the Law of the Sea, Dec. 10, 1982, 1833 U.N.T.S. 397. Enacted as: entered into force as the "United Nations Convention on the Law of the Sea" on Nov.1994. [http://www.un.org/depts/los/convention\\_agreements/texts/unclos/unclos\\_e.pdf](http://www.un.org/depts/los/convention_agreements/texts/unclos/unclos_e.pdf)
3. Donchyts, Gennadii, Fedor Baart, Hessel Winsemius, Noel Gorelick, Jaap Kwadijk, and Nick Van De Giesen. "Earth's surface water change over the past 30 years." *Nature Climate Change* 6, no. 9 (2016): 810. (a)
4. Donchyts, Gennadii, Jaap Schellekens, Hessel Winsemius, Elmar Eisemann, and Nick van de Giesen. "A 30 m resolution surface water mask including estimation of positional and thematic differences using landsat 8, srtm and openstreetmap: a case study in the Murray-Darling Basin, Australia." *Remote Sensing* 8, no. 5 (2016): 386. (b)
5. Gorelick, Noel, Matt Hancher, Mike Dixon, Simon Ilyushchenko, David Thau, and Rebecca Moore. "Google Earth Engine: Planetary-scale geospatial analysis for everyone." *Remote Sensing of Environment* 202 (2017): 18-27.
6. Irazoqui Apecechea, M., Verlaan, M., Zijl, F., Le Coz, C., & Kernkamp, H. (2017). Effects of self-attraction and loading at a regional scale: a test case for the Northwest European Shelf. *Ocean Dynamics*, 67, 729-749.
7. Luijendijk, A., Hagenaaars, G., Ranasinghe, R., Baart, F., Donchyts, G., & Aarninkhof, S. (2018). The state of the world's beaches. *Scientific reports*, 8(1), 1-11.
8. Pekel, Jean-François, Andrew Cottam, Noel Gorelick, and Alan S. Belward. "High-resolution mapping of global surface water and its long-term changes." *Nature* 540, no. 7633 (2016): 418.
9. Richard C. Ausness & Frank E. Maloney, The Use and Significance of the Mean High Water Line in Coastal Boundary Mapping, 53 N.C. L. Rev. 185 (1974).
10. Sagar, Stephen, Dale Roberts, Biswajit Bala, and Leo Lymburner. "Extracting the intertidal extent and topography of the Australian coastline from a 28 year time series of Landsat observations." *Remote Sensing of Environment* 195 (2017): 153-169.
11. Wang, X., Verlaan, M., Apecechea, M. I., & Lin, H. X. (2022). Parameter estimation for a global tide and surge model with a memory-efficient order reduction approach. *Ocean Modelling*, 173, 102011.
12. Wilson, Adam M., and Walter Jetz. "Remotely sensed high-resolution global cloud dynamics for predicting ecosystem and biodiversity distributions." *PLoS biology* 14, no. 3 (2016): e1002415.

## 7 Annex – digital satellite derived coastlines and intertidal areas

The satellite derived coastlines and dataset that delineates the inter-tidal areas of Europe as determined and described in this report are available for viewing and for downloading as digital files in shape format. Therefore, these coastlines and inter-tidal areas have been added as an extra Bathymetry layer in the Central Viewing Service at the EMODnet portal (<https://emodnet.ec.europa.eu>). Look under EMODnet bathymetry in the Catalogue. The coastlines are given for the three most used levels, i.e. Lowest Astronomical Tide (LAT), Mean Sea Level (MSL) and Mean High Water (MHW). The inter-tidal area is derived as the area between the coastlines at MHW and LAT. The extra layer is also included in the WMS-WFS service.